Interdiffusion at Interfaces of Polymers with Dissimilar Physical Properties

Jae-Myeong Jung and Hyungsuk Pak

Department of Chemistry, Seoul National University, Seoul 151-742, Seoul Korea
Received February 12, 1997

The interface between two different polymers is characterized theoretically by using a model. This model is based on the assumption that the monomeric friction coefficients of the two polymers are identical but a strong function of the matrix composition. This model predicts that the concentration profiles are highly asymmetric with substantial swelling of the slower-diffusing component by the faster component. To predict the behavior of interdiffusion, three quantities are used: distance of interface $Z^*(t)$ due to the swelling, interfacial width $W(t)$ which is most sensitive to the detailed composition profiling, and mass transport $M(t)$ due to interdiffusion. It is found that the more dissimilar polymer pairs, the faster the movement of the interface, the quicker its interfacial width saturates to a limiting value and the slower its mass transport. These results are in qualitative agreement with some experiments.

Introduction

Interdiffusion of polymeric molecules is important in diverse areas of polymer science, ranging from 'tack' of rubber and crack healing in glassy polymers to the kinetics of phase separation in polymer blends. The study of interdiffusion in polymeric materials is of concern in numerous fields such as the encapsulation of microelectronics devices, rubber-toughened polymer composites, processing of polymer blends, dynamics of phase separation in polymer mixtures, polymer adhesion and welding of polymer interfaces, kinetics of adhesion, and coating. Understanding the diffusion processes in polymers is the key to successful production of polymers and application of polymer products in industry. Due to relatively slow relaxation processes of polymer chains in comparison to systems of small molecules, polymers also offer the ideal systems for fundamental studies of diffusion and kinetics of spinodal decomposition. The examination of the interdiffusion between different species of polymers has great practical relevance and academic significance. However, due to the rich equilibrium phase behaviors found in polymeric systems, ranging from miscibility and crystallization to glass transition, diffusion complicate this subject of interdiffusion to a spectacular degree.[1,2] Polymer/polymer interdiffusion affects the mechanical properties of polymers near the interface. The final properties of polymers are determined by the thickness of the interface or by the concentration profile of the two polymers across the interface. The interdiffusion process at a polymer/polymer interface is a strong function of temperature, composition, compatibility, molecular weight, molecular-weight distribution, chain orientation, and molecular structures. In particular, differences in physical properties of the two polymers have marked effects on the shape of the concentration profile during the interdiffusion process. For example, Brochars-Wyart and de Gennes[3,4] showed that in asymmetric conditions polymers reptate in a moving tube. E. Jabbari *et al.*[5] showed experimentally that polymer pairs with dissimilar physical properties can be highly asymmetric in the concentration profile.

In the experiments on this subject, a thin film of polymer species A is placed in contact with another polymer species B film. The evolution of the initially sharp boundary between A and B is monitored with respect to time by various experimental techniques. If polymers A and B are compatible, the initial sharp interface will be smeared out as a result of the ordinary Fickian type diffusion. The situation is somewhat more delicate and interesting when polymers A and B are only partially miscible, *i.e.* when the ambient temperature is in the biphasic region. Klein and co-workers have obtained direct measurements of time-dependent composition profiles at an interface between two partially miscible polymers A and B (dPS: deutrated polystyrene /PS: polystyrene).[6,7] In particular, interfacial broadening with elapsing time was studied in detail. With the interfacial width $W(t)$ defined as related to the reciprocal of the maximal composition gradient across the A/B boundary, it was found that the thickness of the interface $W(t)$ increases with time slower than that expected from a Fickian process of $W(t) \propto t^{1/2}$. Since the interdiffusion process is driven by thermodynamic forces,[8] as the opposite of the phase separation, the transport phenomena in the bilayer were expected and found experimentally to depend strongly on thermodynamic conditions such as temperature, interaction parameter between polymers A and B, and molecular weights of A and B. In the experiment of Steiner *et al.*,[7] where interfacial relaxation took place between polymer A-rich and polymer B-rich layers prepared with coexisting compositions, the exponent α in a scaling law $W(t) \propto t^{\alpha}$ was found to be considerably smaller than the Fickian exponent 1/2, falling between 0.25 and 0.5. Yet the experiment could not exclude the possibility that deeper in the two phase region the exponent α might be smaller than 0.25, since the experiment was not performed far away from the critical temperature for miscibility. The definition of maximal gradient adopted in studies of Steiner, U. *et al.*[6,7] is very sensitive to the local structure of the interface (We will use a new definition of $W(t)$, based on these studies of Steiner, U. *et al.*).

The interdiffusion process can also be described meaningfully by observing $M(t)$, the amount of species A transported across the initial boundary separating A and B as a

function of time: $M(t) \propto t^{\beta}$. This definition of $M(t)$ is extremely insensitive to the local structure of the composition profile and hence can be used to describe an interdiffusion process in the most unambiguous way. In addition, it permits the highest degree of precision in the experimental determination of exponent β. Interdiffusive behaviors of polymer mixtures can be characterized as following the temporal changes of both maximal gradient in spatial distribution of composition and mass transport across the interface. We believe that both the interfacial width $W(t)$ and mass transport $M(t)$ are required in order to obtain a more sophisticated description of interdiffusion between polymer blends.

On the other hand, Kramer and associates[9,10] showed that, for polymer pairs with different molecular weights, the interface moves towards the polymer with a lower molecular weight as interdiffusion proceeds. Kramer *et al.*[11] and Sillescu[12] described the interdiffusion in systems with a moving interface due to unequal fluxes of polymers A and B, which were balanced by a net flux of vacancies across the interface. By assuming the chemical potential of vacancies to be zero in the melt state but the flux of vacancies to be finite, they derived the following equation for the interdiffusion coefficient:

$$D = \phi_A \phi_B \left(\frac{\phi_B}{\phi_A} \Lambda_A + \frac{\phi_A}{\phi_B} \Lambda_B \right) \left(\frac{1}{N_A \phi_A} + \frac{1}{N_B \phi_B} + 2\chi \right) \quad (1)$$

Here, D is the interdiffusion coefficient; Λ_A and Λ_B are the mobilities of polymers A and B, respectively; N_A and N_B are the number of repeat units of each polymer; ϕ_A and ϕ_B are the mole fractions of each polymer; and χ is the Flory-Huggins interaction parameter. In the theory, the overall mobility is linearly related to the mobility of each component, indicating that the interdiffusion coefficient is dominated by the faster-moving component. Akcasu *et al.*[13] observed the diffusion behaviors in dynamic scattering experiments with ternary polymer solutions. They defined the vacancies as the third component in a mixture of A and B polymers and concluded that the fast-mode was obtained in the limit of high vacancy concentration or a matrix with very high mobility. Since the polymer mobility and the vacancy concentration are high above T_g, it is inferred that the theories concerned describe the interdiffusion above T_g. In fact, most of the interdiffusion data in the literature[14] which were collected above the T_g of polymers are consistent with the fast-mode theory of interdiffusion. Kramer *et al.*[11] used Rutherford backscattering spectroscopy to follow the movement of a gold marker at the interface between PS and d-PS with different molecular weights. Reither *et al.*[15] used X-ray reflection spectrometry for the same purpose. They observed the movement of the interface toward the faster diffusion component. Recent results from Sauer and Walsh[2] and E. Jabbari *et al.*[5] have shown that, for polymer interfaces with dissimilar properties, the faster diffusing component swells the slower diffusing component at temperature near the T_g of the slower diffusing polymer. These results were obtained by using a polymer pair consisting of PS as the slower diffusing component with a T_g of 101 °C and PVME (poly(vinyl methyl ether)) as the faster diffusing component with a T_g of −27 °C. The concentration profile was highly asymmetric. Composto and associates[16] investigated interdiffusion in a polymer pair consisting of PS as the faster-diffusing component with a T_g of 105 °C and PXE (poly (xylenyl ether)) as the slower-diffusing component with a T_g of 216 °C. Their results show that the concentration profile for this polymer pair is also asymmetric with the swelling of the slower-diffusing component, PS(Fig 7b). Defining the interface position x_i, as the depth at which ϕ_{PXE}=0.5, they showed that the interface-shift Δx_i, relative to the position of the interface at t=0, was increased linearly with t^{α} at all diffusion temperatures. The characteristics of Δx_i, which we will define as $Z^*(t)$, are also required for a precise description of the interdiffusion between polymer blends. As discussed below, this non-Fickian profile must be due to the strong concentration dependence of the mutual diffusion coefficient. For interdiffusion at homopolymer interfaces or interfaces between polymers with similar physical properties, the mobilities are relatively independent of composition across the interfaces. However, for polymers with dissimilar physical properties, the composition dependence of the mobilities has a significant effect on the concentration profile. Since the matrix is homogeneous on a microscopic scale for many polymers, there exists a relationship between the polymer mobilities that relates these mobilities to the properties of the matrix.

Here we present a model for interdiffusion at polymer/polymer interfaces for polymers with similar and very dissimilar properties. This model is based on irreversible thermodynamics and accounts for the composition dependence of the tracer diffusion coefficients of the two polymers which are identical but a strong function of composition. The composition dependence of the monomeric friction coefficients is calculated approximately from the many experimental data for polymer blends. In addition, we consider the Cahn-Hilliard interfacial energy associated with the spatial variation of the composition at the interface during the interdiffusion of polymers.

Theory

Description of the System. For our model, a simple system is considered: The interdiffusion pair is schematically shown in Figure 1. One phase consists of the polymer with low mobility (designated by *s* for "slow") with vacancies randomly distributed on the lattice. The other phase consists of the polymer with high mobility (designated by *f* for "fast"). It is assumed that the concentration of vacancies is a small fraction of the total concentration and does not contribute to the free energy of mixing. Since the polymers on each side of the interface have different molecular weights and chemical structures, there is a chemical potential gradient across the interface. The system is modeled by using this chemical potential gradient as the driving force for interdiffusion and by taking the assumption of quasi-equilibrium on a microscopic scale, which means that the polymer molecule is at equilibrium locally while interdiffusion takes place.

Irreversible Thermodynamic Formulation. We adopt the Onsager formulation,[17,18] which relates the flux of the species across the interface to the chemical potential gradient of each component:

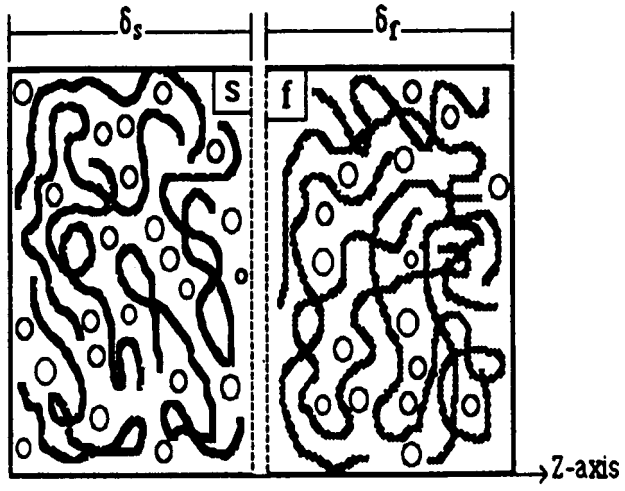

Figure 1. Schematic diagram of the interdiffusion pair consisting of the polymers with low mobility (*s*=slow) and high mobility (*f*=fast) with vacancies (○) distributed randomly in the lattice.

$$j_i = \frac{-1}{RT}\sum_k \Lambda_{ik}\nabla\mu_k \quad i,k = s,f,v \qquad (2)$$

Here, subscripts *s*, *f*, and *v* stand for slow component, fast component and vacancies, respectively. The symbol j_i, a scalar, is the molar monomeric flux of component *i* for one-dimensional diffusion; *T* is the absolute temperature; *R* is the gas constant; μ_k is the molar monomeric chemical potential of component *k*; Λ_{ii} is the Onsager coefficient of component *i*; and Λ_{ik} is the cross-coefficient of component *i* due to the gradient of component *k*. In the above equations, the Onsager reciprocity relations[18] are used to reduce the number of Onsager coefficients from nine to six. From one-dimensional diffusion in the Cartesian coordinate system with negligible excess volume of mixing and no change in the lattice size, the sum of the three fluxes must be equal to zero:

$$j_s + j_f + j_v = 0 \qquad (3)$$

This relationship can be used to express the vacancy Onsager coefficients in terms of the coefficient of the other two components:

$$\Lambda_{iv} = -\sum_j \Lambda_{ij} \quad i = s,f,v \quad j = s,f \qquad (4)$$

Substituting for vacancy Onsager coefficients from Eq. (4) and neglecting the cross-coefficients results in the following relation between the fluxes and the chemical potential gradients:

$$j_i = -\frac{\Lambda_{ii}}{RT}\nabla(\mu_i - \mu_v) \quad i = s,f \qquad (5)$$

$$j_v = \sum_i \frac{\Lambda_{ii}}{RT}\nabla(\mu_i - \mu_v) \quad i = s,f \qquad (6)$$

If the chain relaxation time has the same order of magnitude as the experimental time, then the chemical potential of vacancies is negligible. The experimental results of E. Jabbari *et al.*[19] from interdiffusion of a two-physically-different-polymer pair (PS/PVME) above the T_g of slower diffusion component PS, indicate that the diffusion process is independent of the molecular weight of PS on the assumption that the chemical potential of vacancies is negligible. Assuming that the vacancy concentration is nearly at equilibrium everywhere, the chemical potential of vacancies is negligible compared with the chemical potential gradient across the interface:

$$\nabla\mu_v = 0 \qquad (7)$$

then, Equation (5) reduces to the following:

$$j_i = -\frac{\Lambda_{ii}}{RT}\nabla\mu_i \quad i = s,f \qquad (8)$$

Chemical Potential Gradient. It is known that equilibrium properties of a polymer mixture of spatially uniform composition can be approximately described by the Flory-Huggins type lattice theory.[20] The Flory-Huggins equation is used to relate the chemical potential to the entropy and enthalpy of mixing of the two polymers. When the mixture phase separates, interfaces are created between two or more phases. At phasic boundaries, polymer chains rearrange their conformations and repel chains of dissimilar species. This leads to an increase in free energy of both entropic and enthalpic origin. Now the total free energy will take a generalized form:

$$F = \int dV\left[f_0(\phi) + \left(\frac{k}{4}(\nabla\phi)^2\right)\right] \qquad (9)$$

where f_0 is the free energy density of the system, and the second term involving $(\nabla\phi)^2$ accounts for the Cahn-Hilliard interfacial energy associated with the spatial variation of the composition. The phenomenological parameter κ has the dimension of length squared and plays an important role in control and formation of interfaces. It is generally a function of concentration ϕ and should also depend upon specific properties of both polymer species as well as ambient temperature. In the Flory-Huggins theory for incompressible polymer mixtures of lengths N_s and N_f, f_0 is given by the familiar expression

$$f_o = \left(\frac{\phi}{N_s}\right)\ln(\phi) + [(1-\phi)/N_f]\ln(1-\phi) + \chi\pi(1-\phi) \qquad (10)$$

with ϕ being the volume fraction of polymer *s*. Since N_s and N_f are large and the entropy of mixing is very weak and relatively small, positive Flory χ parameter is sufficient to make *s* and *f* phases separate into *s*-rich and *f*-rich phases. The polymer-vacancy interaction parameter is negligible. This is a good assumption since the concentration of vacancies is an order of magnitude lower than the polymer concentration. Then,

$$\phi_s + \phi_f = 1 \qquad (11)$$

In general, depending on the initial conditions, polymers *s* and *f* may either demix through spinodal decomposition or interdiffuse into each other. Phase separation cannot be perfect when the system is not far enough from the critical point for miscibility. By the same token, partial mixing *via* interdiffusion will occur when a layer of pure polymer s is

put in contact with a layer of pure *f*, but the diffusion is not free in the sense of Fickian transport, and anomalous behaviors are anticipated. Since a complete mixing is prevented by thermodynamics, the interface between *s* and *f* presents a diffusion barrier where the composition crosses over from its coexistence value of one phase to that of the other. Consequently, the diffusion constant is negative at the middle of the interface where the interfacial effect stabilizes the interdiffusion process. In our situation, the initial arrangement is a sharp contact between two unmixed polymer species *s* and *f*. The thermodynamic driving forces, both from the bulk and interfacial region, compel the system to mix through the interfacial region.

The equilibrium theory of Helfand and others[21,22] for the interfacial structure of polymer blends also produces a simple expression for the parameter $\kappa(\phi)$ in

$$\kappa(\phi)=\frac{\sigma_s}{\phi}+\frac{\sigma_f}{1-\phi} \tag{12}$$

where σ_s, σ_f are the size of subunit. In the case of $\sigma_s=\sigma_f=a^2$

$$\kappa(\phi)=\frac{a^2}{\phi(1-\phi)} \tag{13}$$

where *a* is a monomer length.

Then, the molar monomeric chemical potential for each component is obtained from the functional derivative of total free energy with respect to the number of moles of that component,

$$\mu=\frac{\delta F}{\delta\phi}=\frac{\ln\phi+1}{N_s}-\frac{\ln(1-\phi)+1}{N_f}+\chi(1-2\phi)-\frac{a^2}{2\phi(1-\phi)}\nabla^2\phi \tag{14}$$

whereas the chemical potential gradient is obtained from the derivative of monomeric chemical potential with respect to the diffusion axis:

$$\nabla\mu_i=\nabla\left(\frac{\delta F}{\delta\phi_i}\right) \tag{15}$$

$$\nabla\mu_i=\left(\frac{1}{\phi_s N_s}+\frac{1}{(1-\phi_s)N_f}-2\chi_{sf}\right)\nabla\phi_i-\frac{a^2}{2\phi_s(1-\phi_s)}\nabla^3\phi_i \tag{16}$$

Here, χ_{sf} is the interaction parameter between a monomer of the slower and faster moving components, and N_s and N_f are the number of repeat units for the slower and faster moving components, respectively. Equation (16) relates the monomeric chemical potential gradient of each component to temperature, molecular weight of each polymer, compatibility parameter and composition. In arriving at Eq. (16), we have neglected nonlinear terms involving $(\nabla\phi)^3$ and $(\nabla\phi)\nabla^2\phi$. These terms are unimportant at late stages of interdiffusion when the interface has sufficiently broadened.

Since the polymers are incompressible, the net exchange of matter across the interface as a result of different diffusion coefficients of the two polymers causes swelling of the slower diffusing component by the faster moving component. This swelling results in the movement of the interface as interdiffusion progresses. The amount of swelling is related to the net flux of vacancies across the interface. Therefore, the total flux of each component is given by the following relations:

$$j_i^I=j_i+\phi_i j_v \qquad i=s,f \tag{17}$$

The total flux j_s^I of s across a plane fixed with respect to the coordinate system is the sum of the diffusion flux of *s* and the *s* transported by the vacancy flux, then:

$$j_s^I=-[(1-\phi_s)\Lambda_s\nabla\mu_s-\phi_s\Lambda_f\nabla\mu_f] \tag{18}$$

here, j_s^I and j_f^I, scalar quantities, are the total molar monomeric flux of the slower- and faster-diffusing components, respectively.

The Onsager Coefficients. One topic in studies of interdiffusion is to derive the functional form of $\Lambda(\phi)$ at a phenomenological level by setting the off-diagonal Onsager coefficients to zero.[11,23,24] Recently some Monte Carlo simulations also have been carried out.[25] But, there has not been any attempt to formulate the transport coefficient $\Lambda(\phi)$ at molecular-level. De Gennes[3] has shown that the Onsager coefficients for interdiffusion of polymer *i* due to a gradient of its own chemical potential, Λ_{ii} are given by the following equation:

$$\Lambda_{ii}=\frac{1}{f_i^m\Omega}\frac{N_i^e}{N_i}\phi_i(1-\phi_i) \quad i=s,f \tag{19}$$

Here, f_i^m is the monomeric friction coefficient of component *i* as if it is a Rouse chain; N_i^e is the number of repeat units between entanglements for component *i*; ϕ_i is the molar fraction of polymer *i*; and Ω is the volume of a quasi-lattice site assumed to be the same for both molecules, respectively. Roland and Ngai[26] measured the segmental relaxation in a two-physically different polymer blend, PS/PVME, using dielectric spectroscopy. According to their results there was a significant coupling and intersegmental cooperativity in the relaxation spectrum of this blend. This clearly indicates that the mobility of a chain in the polymer blend matrix is strongly influenced by the other component and suggests that the friction coefficients, f_s^m and f_f^m should be identical but a strong function of the matrix composition. Therefore, for compatible polymer pairs, Eq. (19) reduces to the following:

$$\Lambda_{ii}=\frac{1}{f^m\Omega}\frac{N^e}{N_i}\phi_i(1-\phi_i) \tag{20}$$

Here, f^m is the molar monomeric friction coefficient for the blend, which is strongly composition-dependent for a polymer pair with dissimilar physical properties. The parameter N^e is the average number of repeat units between entanglements for the blend. In a E. jabbari *et al.*'s paper,[27] they have suggested a model for interdiffusion at interfaces of polymers with dissimilar physical properties, such as PS/PVME. In that, they evaluated the composition dependence of the monomeric friction coefficient from the blend zero shear viscosity using the reptation theory. They predict that the concentration profiles are highly asymmetric, with substantial swelling of the slower diffusing component by the faster diffusing component.

The model presented in our study is based on the assumption that the tracer diffusion coefficient of the two po-

lymers is strongly coupled to the properties of the matrix. Thus, the chain diffusion coefficient is related to the chain molecular weight, the mesh size of the entangled chains and the composition of the matrix, and is relatively independent of the monomer structure of the diffusing chain. For simplicity, we will take some reasonable approximations based on the empirical results.

Flux of Each Component. Substituting the fluxes from Eq. (2) and the chemical potential gradients from Eq. (16) and the Onsager coefficients from Eq. (20) into Eq. (17) results in a relation between the total flux of the slower-diffusing component and the molecular parameters of each polymer:

$$j_s^i = -\left(\frac{N^e}{f^m \Omega}\right)\left(\frac{(1-\phi_s)}{N_s}+\frac{\phi_s}{N_f}\right) \left[\left(\frac{(1-\phi_s)}{N_s}+\frac{\phi_s}{N_f}-2\chi\phi_s(1-\phi_s)\right)\nabla\phi_i - \frac{a^2}{2}\nabla^3\phi_i\right] \quad (21)$$

It is possible to describe this transport process by simply applying the law of mass conservation. According to the conservation law, the temporal change of composition in space can be described by the dynamic equation. For the bilayer arrangement in Figure 1, the analytical description reduces to a one-dimensional space denoted by the z-axis. For conservation of s-segmental, molar balance for each component results in the following equation relating the rate of flux as a function of distance to the rate of change of concentration as a function of time:

$$\frac{\partial\phi_s}{\partial t} = -\Omega\frac{\partial j_s^i}{\partial z} \quad (22)$$

where Ω is the volume of quasi-lattice site. The time and spatial dependence of the mole fraction of the slow component can be obtained by substituting the total flux from Eq. (21) into Eq. (22):

$$\frac{\partial\phi_s}{\partial t} = \frac{\partial}{\partial z}\left\{\left(\frac{N^e}{f^m\Omega}\right)\left(\frac{(1-\phi_s)}{N_s}+\frac{\phi_s}{N_f}\right) \times\left[\left(\frac{(1-\phi_s)}{N_s}+\frac{\phi_s}{N_f}-2\chi\phi_s(1-\phi_s)\right)\nabla\phi_i - \frac{a^2}{2}\nabla^3\phi_i\right]\right\} \quad (23)$$

The above equation relates the time and spatial dependence on the slower diffusing component to molecular properties such as molecular weight, compatibility parameter, temperature and the blend friction coefficient. The first term of Eq. (23) accounts for the mobility of the polymer chains via the monomeric friction coefficient f^m, the second term accounts for the differences in molecular weights of the two polymers, and the factor in the front of the third term accounts for the free energy of mixing. The other major difference from an ordinary Fickian diffusion equation is that the third term can turn negative, amounting to a negative diffusion constant and therefore "uphill diffusion". The forth term involving $\partial^3\phi/\partial z^3$ accounts for the presence of an interface separating two incompatible phases. If the two polymers have similar physical properties but different molecular weights, then the second term is the dominant term, as in the case of the fast-mode theory.[11,12] However, if the two polymers have widely different physical properties, then the first term dominates.

Now, consider the calculation of the molar monomeric friction coefficient, f^m. From many experimental data, we can find that the composition dependence of the monomeric friction coefficient for the polymer pair is nearly linear in logarithmic scale (Figure 2). Green *et al.*[28] measured the tracer diffusing coefficient of PS in PS/PVME matrices of different composition with forward recoil spectrometry and they evaluated the matrix composition using the reptation theory. In Figure 2, this variation of the monomeric friction coefficients with composition is shown. The blend monomeric friction coefficient has changed by six orders of magnitude through the composition variation from pure PS (the volume fraction of the slower diffusing component PS, ϕ_s=1) to pure PVME (ϕ_s=0). As PVME is added to a PS matrix, the friction coefficient decreases dramatically owing to the high mobility and the low T_g of PVME and the friction coefficient becomes dominated by the physical properties of PVME. This indicates that PVME plasticizes the PS matrix as interdiffusion takes place across the interface. Therefore, for polymers with dissimilar physical properties, interdiffusion is accompanied by the swelling of the slower diffusing component. In Figure 2, the dotted line is our approximate line representing the linear relation between logarithmic scale of monomeric friction coefficient, f^m and volume fraction of each component. So, f^m can be expressed by:

$$\begin{aligned} -\log f^m &= G(1-\phi_s)+const \\ f^m &= \exp[-G(1-\phi_s)-const] \\ &\propto \exp(G\phi_s) \end{aligned} \quad (24)$$

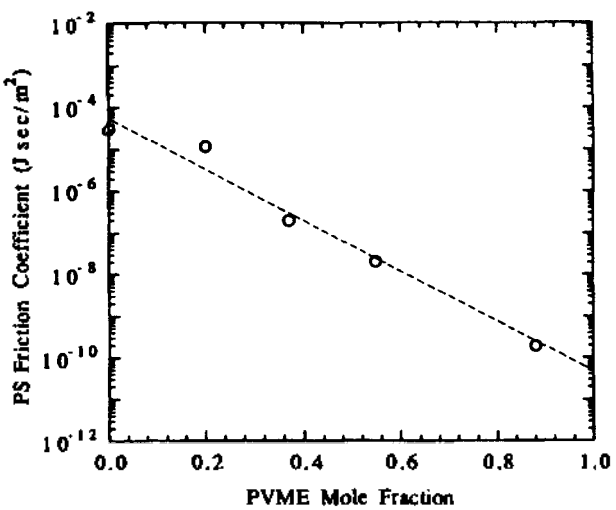

Figure 2. Experimental (open circles) monomeric friction for the PS/PVME pair at 120 °C. These data points were extracted from Green *et al.*[36] with PS and PVME average Mw of 1.05×10^5 and 9.9×10^4 and polydispersity indices of 1.06 and 2.10, respectively. The dotted line is our approximate line representing the linear relation between logarithmic scale of monomeric friction coefficient f_i^m and volume fraction of each component.

where G is the slope of the dotted line in Figure 2 and is the value related to the degree of difference in the monomeric friction coefficient of each polymer component. A greater value of G means that the polymer pairs will be more dissimilar in component. On the other hand, the number of repeat units between the entanglements for the blend can be estimated from the relationship between the entanglement molecular weight and the plateau modulus.[29]

$$\frac{1}{N_e}=\left(\frac{\phi_s}{(N_s^e)^{1/2}}+\frac{\phi_f}{(N_f^e)^{1/2}}\right)^2 \tag{25}$$

In general, the entanglement molecular weight of most polymers has the same order of magnitude. So, we can assume by approximation that N^e is independent of composition. Then, we can obtain the following equation:

$$\frac{\partial\phi_s}{\partial t}=\frac{\partial}{\partial z}\left\{D\times\exp(-G\phi_s)\left(\frac{(1-\phi_s)}{N_s}+\frac{\phi_s}{N_f}\right)\right.$$
$$\left.\times\left[\left(\frac{(1-\phi_s)}{N_s}+\frac{\phi_s}{N_f}-2\chi\phi_s(1-\phi_s)\right)\nabla\phi_i-\frac{a^2}{2}\nabla^3\phi_i\right]\right\} \tag{26}$$

where D is a constant including N^e. We define $R=r-1$ using the polymerization ratio $r=N_s/N_f$; the interfacial parameter K to have the magnitude of the square of the radius of gyration: $K=N_sa^2$; and we have also made a change of notation: $N=N_s\chi$. We scale length by the natural length $K^{1/2}$ in the problem and make the conversion $z\rightarrow z/K^{1/2}$. We scale time with the unit $\tau=2K(N_s)^2/D$, which is on the order of the reptation time of a single chain in a melt, and make the transformation $t\rightarrow t/\tau$. Rewriting the resulting Eq. (26) in terms of the rescaled variables, we find:

$$\frac{\partial\phi_s}{\partial t}=\frac{\partial}{\partial z}\{\exp(-G\phi_s)(1+R\phi_s)$$
$$\times[(2+(2R-4N)\phi_s+4N\phi_s^2)\nabla\phi_i-\nabla^3\phi_i]\} \tag{27}$$

Boundary Conditions. As long as the mass transport has not approached the outer two boundaries of the thin film, the interdiffusion process can still be described by Eq. (27). The initial and boundary conditions to solve the above diffusion equation are:

$$\begin{array}{lll} t=0 & \phi_s=0 & \\ t=0 & \phi_s=1 & \text{for } \begin{array}{l}0\le z<\delta_f\\ \delta_f\le z<\delta_s+\delta_f\end{array}\end{array} \tag{28a}$$

$$\begin{array}{lll} z=0 & \dfrac{\partial\phi_s}{\partial z}=0, & \dfrac{\partial^3\phi_s}{\partial z^3}=0 \\ z=\delta_s+\delta_f & \dfrac{\partial\phi_s}{\partial z}=0, & \dfrac{\partial^3\phi_s}{\partial z^3}=0 \end{array} \quad \text{for } t>0 \tag{28b}$$

where we set the film length $\delta_s=\delta_f=0.5$ in order to normalize the full film length. The boundary conditions of the Eq. (28b) represent no-flux boundary conditions. In Eq. (28a), we take $\phi_s=0$ and $\phi_s=1$, which is a step function as corresponding to phases which are 100% *f*-rich and *s*-rich at $t=0$, respectively. This situation in the condition is described in Figure 1. For the polymer pair with dissimilar properties the differential equation becomes stiff and the second initial condition of Eq. (28a), is a measure of the stiffness for the differential equation.

Numerical Method

It is not feasible to seek the analytical solution of the nonlinear partial differential equation of Eq. (27). But numerical solutions can be obtained by discretizing Eq. (27) with finite differences. Consider the situation namely, a bilayer of initially pure polymer *s* and polymer *f*. Regarded as a one-dimensional problem, the left-hand side is occupied by *f* and the right-hand side by *s* initially. The evolution of the bilayer system starting from the initial profile of a step function is described by the application of the standard Crank-Nicholson method to update at every time step the profile described by Eq. (27). In discretizing $\partial\phi(z,t)/\partial t$ term as $(\phi_i^n-\phi^{n-1}{}_i)/\Delta t$, $\partial\phi(z,t)/\partial z$ as $(\phi^n{}_{i+1}-\phi^n{}_{i-1})/2\Delta z$, and similarly for its higher spatial derivatives, Δt is chosen as $\Delta t=10^{-8}$ and a grid point Δz as $\Delta z=10^{-5}$. We transform many nonlinear terms, such as $\nabla\phi$, $\nabla^2\phi$, $\nabla^3\phi$, $\nabla^4\phi$, and their products, into linear terms using the Newton method. Our differential equation is solved with a variable-step-size finite-difference method. We allow the system to evolve 50000 time steps as far as the boundary condition will remain valid.

Result and Discussion

As discussed in the Introduction, we consider three quantities, one reflecting the local structure at the middle of the interface and others depicting the overall profile of the composition field, in order to provide a reliable description of the interdiffusion process. Now we define the interfacial width $W(t)$ for our model, in the form similar to the definition of ref 6; namely, we define new $W(t)$ in terms of the maximal gradient of composition. For a case such as the present study, $W(t)$ is simply given by

$$W(t)=\left[\left(\frac{\partial\phi(z^*,t)}{\partial z}\right)^{-2}-\left(\frac{\partial\phi(z=100\Delta z,t=0}{\partial z}\right)^{-2}\right]^{1/2} \tag{29}$$

where z^* is the value of z at $\phi=0.5$, and '$z=100\Delta z$' is the initial interface position since we take 200 grid points in the interface-around area. $W(t)$ is given on unit of $K^{1/2}$. Because of the suppressed diffusion due to the "spinodal barrier", it is expected that the exponent α in the power law $W(t)\propto t^{\alpha}$, does not exceed 0.5. Moreover, the value of α does not have to stay between 0.25 and 0.5 since the existence of an optimal stationary interfacial width is plausible in a steady-state of interdiffusion.

Another characteristic property is the mass transport $M(t)$ of polymer *f* transported from the left-hand side of the interface to the right. $M(t)$ is calculated according to

$$M(t)=\varepsilon\times\int_{100\Delta z}^{200\Delta z}dz\ \phi_f(z,t) \tag{30}$$

where ε is a constant and $\phi_f=1-\phi_s$ in according to Eq. (11). Since we are concerned with the narrow area around the initial interface, only 100 grid points (100 Δz's) from each side (from the slower and faster sides) around the initial in-

terface are considered. At t=0, the range of grid points from 100th Δz to 200th Δz is occupied only by the slower diffusing component. It is expected that $M(t)$ will increase with time slower than $t^{1/2}$ for the dissimilar couples of polymer blends.

And the last property of the interdiffusion process examined in the study is the distance of interface $Z^*(t)$, from the initial interface position at t=0. It is expected that $Z^*(t)$ also will increase with time slower than $t^{1/2}$ for the case of partially miscible couples of polymer blends. That is, the diffusion is not free, with the system inside the two-phase region.

It is necessary to consider χ_c, which is the value of the Flory interaction parameter χ at the critical temperature T_c. In the Flory-Huggins mean-field model of polymer mixing, χ_c can be expressed by

$$\chi_c = (\sqrt{N_s} + \sqrt{N_f})^2 / 2N_sN_f \tag{31}$$

for the case N_f=N_s, *i.e.*, R=r-1=0 and N_c=$N_s\chi_c$=2, and for the case $2N_f$=N_s, *i.e.*, for R=1, N_c=2.914. One expects to observe the interface broadening and eventual relaxing to its equilibrium dimension, as experimentally found in ref 7. In fact, at a given temperature, *i.e.*, for a given χ, the two phases will coexist in equilibrium with compositions determined by two roots of the following equation:

$$\ln \frac{\phi}{(1-\phi)^{R-1}} + N(1-2\phi) - R = 0 \tag{32}$$

which corresponds to the state μ=0, where μ is obtained from the energy of the Flory-Huggins lattice theory. In our model N=2 for R=0 and N=3 for R=1 are used to have the situation near the critical point.

By this numerical analysis, we can obtain the following results. First, the concentration profile can be obtained. In Figure 3, the simulated concentration profile for R=0 (polymerization ratio is 1, N_s=N_f), N=2, and G=0, at consecutive times after onset of the interdiffusion is shown. The step function is the initial condition which describes the contacted polymer pairs. The time is expressed in scaled units of $2K\ (N_s)^2/D$ and the length in scaled units of $K^{1/2}$. The polymers begin to diffusing into each other side. Since it is the case of very similar polymer pairs, the time evolution of the concentration profile is almost the Fickian type, that is, the transport phenomenon appears almost the Fickian. In fact, the full range of z in the above figure is very narrow compared to the width of the thin films of both polymer (that is, 0.001% of the entire width, $\delta_s+\delta_f$ since the full range of the system is normalized to 1). In this figure, the Fickian characteristics are shown as anticipated. To quantify our analysis, we calculate the interfacial width $W(t)$ as a function of time. In Figure 4, this characteristics are described by means of the time evolution of interdiffusion width $W(t)$, since the process can be inspected more clearly by searching for a scaling law $W(t) \propto t^{\alpha}$. And we can find the linear relation in the plots of $\log[W(t)]$ versus $\log(t)$. The best expression of the power-relation is $t^{0.461}$, and the exponent α (the slope in the plots) is found to be 0.461<0.5, which is smaller than the Fickian characteristic value of exponent α, as expected. Next, we calculate the time dependent of $M(t)$. In Figure 5, the linear logarithmic scaled relation with the time evolution of $M(t)$ is shown, which is very similar to $W(t)$ in form and the exponent β (the slope of the plots) is 0.4588 according to the scaling law $M(t) \propto t^{\beta}$. It also resembles the Fickian characteristics. Since the curves are not straight lines throughout all the time interval in either Figure 4 or Figure 5, power laws such as $W(t) \propto t^{\alpha}$ and $M(t) \propto t^{\beta}$ hold only for a certain period during the interdiffusion. In this case, the behaviors associated with the interfacial dynamics are relatively similar to those related to mass transport, namely, both quantities, $W(t)$ and $M(t)$, which describe the Fickian-like behavior of interdiffusion for similar polymer pairs.

Now consider the other case, that is, the interdiffusion of

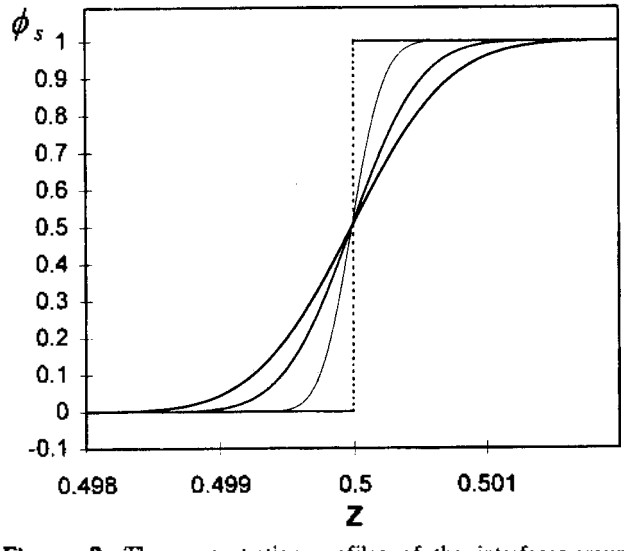

Figure 3. The concentration profiles of the interfaces-around area for G=0, N=2, R=0, at consecutive times. We denote the coordinate perpendicular to the films as z. The initial condition consists of the pure f-film separated from the pure s-film by a sharp interface at z=0.5 This range of z is very narrow compared to the widths of thin films of both polymers (0.001% of the entire width).

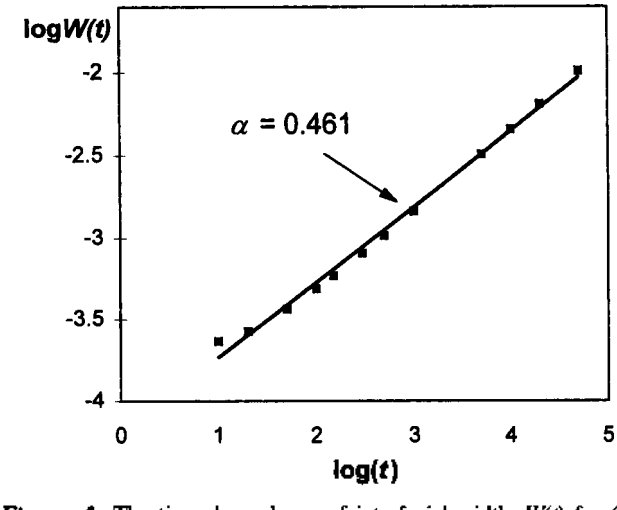

Figure 4. The time dependence of interfacial width, $W(t)$ for G=0, R=0, N=2 plotted in the double-logarithmic form, that is, the plot of $\log[W(t)]$ versus $\log(t)$. The slope α is 0.461. This behavior is almost Fickian characteristics.

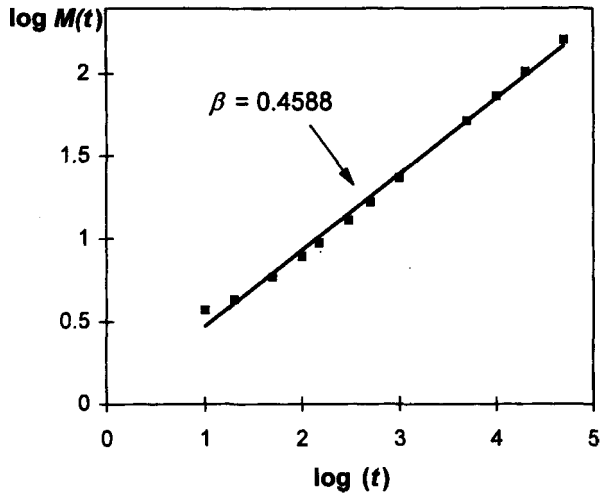

Figure 5. The time dependence of mass transport $M(t)$, for G=0, R=0, N=2 plotted in the double-logarithmic form, that is, the plot of log[$M(t)$] versus log(t). The slope β is 0.4588. This behavior is very similar to $W(t)$ of Figure 4.

polymers with dissimilar physical properties. Comparing this case with the above similar polymer pair case, we find the differences in behavior of the diffusion processes for each property discussed. In Figure 6, the asymmetry of the simulated concentration profile for G=2 predicted by the model is shown. The non-zero value of G signifies that the polymer pairs have different monomeric friction coefficients for each component. This difference is due to the differences in glass temperature T_g, chain length, mobility, etc. According to this figure, the concentration profile for the Fickian model with the constant diffusion coefficient, for we put R=0 and G=0, is symmetric whereas the profile for R=1 and G=2 is asymmetric, with the original interface moving into the slower diffusing polymer layer as a swelling front. It is in good agreement with studies by E. Jabbari *et al.*[27] which indicate that the interface moves as a sharp front into a slower component layer. Time dependence of the concentration profiles for G=1 is shown in Figure 7a. The time evolution of this simulated profile is for t=50τ, 150τ, 250τ and 350τ. This figure shows that the concentration profile remains asymmetric as the interdiffusion proceeds and that the interface moves like a swelling

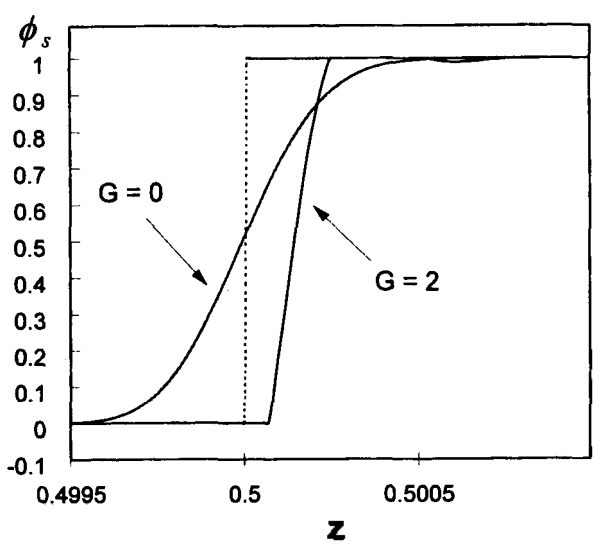

Figure 6. Comparison of the concentration profile for G=2, R=1, N=3 with that for G=0, R=0, N=2 at t=100τ. The dotted curve is the original interface. Different diffusion behavior for each case is described.

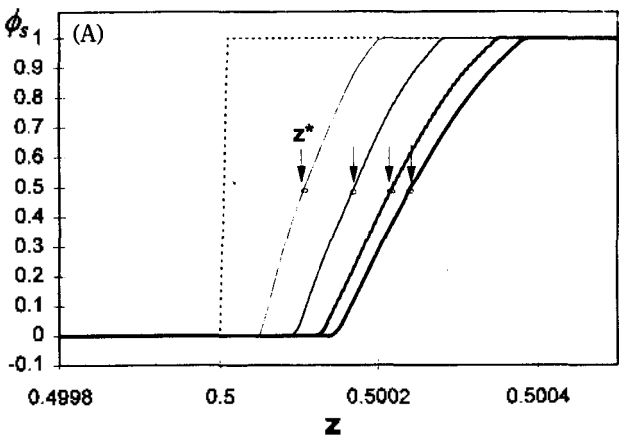

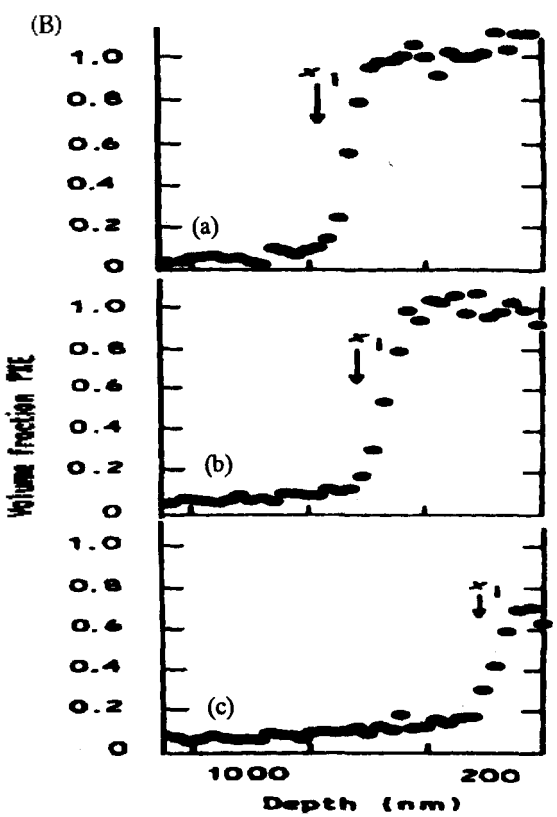

Figure 7. (A) The concentration profiles for G=1, R=1, N=3 at consecutive times (t=50τ, 150τ, 250τ, 350τ). The dotted curve is the original interface and the interfacial movement is shown by remarking z^*. These behaviors are in good agreement with many experimental results (Figure 7B). (B) Composto *et al.*'s experimental volume fraction profile of PXE in the PS/PXE diffusion couple. The couples are heated to 184 °C for (a) 1.0 h, (b) 4.0 h and (c) 16.0 h. The interface position z^* at which ϕ_{PXE}=0.5 is represented (here, expressed by xi).

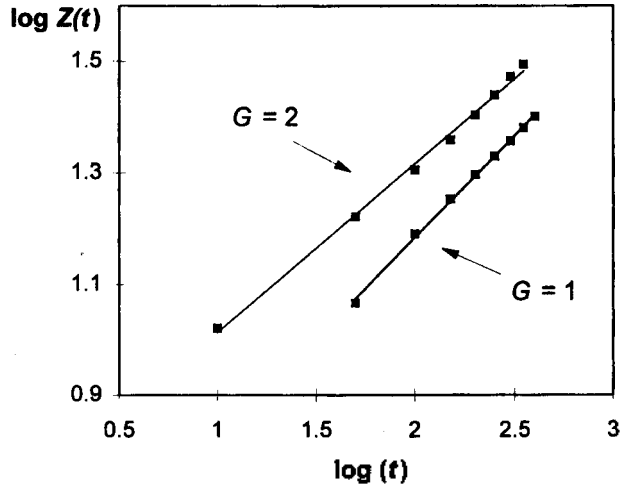

Figure 8. Comparison of the time dependence of the distance of interface $Z^*(t)$ from the initial position, for G=2, R=2, N=3 with that for G=1, R=2, N=3 at consecutive times, plotted in the double-logarithmic form, that is, the plot of log[$Z^*(t)$] versus log(t).

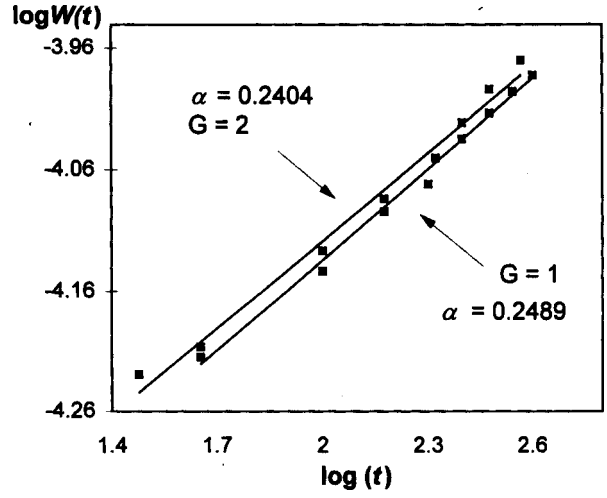

Figure 9. Comparison of the time dependence of the interfacial width $W(t)$ for G=2, R=1, N=3 with that for G=1, R=1, N=3 at consecutive times, plotted in the double-logarithmic form, that is, the plot of log[$W(t)$] versus log(t). The slope α is 0.2404, 0.2489 for G=2, G=1, respectively.

front into the slower component layer. The arrows represent the position of interface defined above as z^* and the movement of the interface can be shown. In this case, we set R=1, which means N_s=2N_f and N=3, in order to obtain a situation near the critical point, instead of one far from the critical point. In accordance with many experimental results, *e.g.*, PS/PXE pair interdiffusion experiment of R. J. Composto and E. J. Kramer (Figure 7b), the interface moved as a sharp front into the slower component side (in the experiment of Figure 7b, PXE is the slower component than PS). This movement is due to the swelling of the slower component by the faster component. In the comparison of the two figures (Figure 7a and 7b), the good agreement between the simulated concentration profile and the experimental data can be found. So by using this model the behavior of interdiffusion in this kind of polymer pairs can be described. In Figure 8, the time evolution of the distance of interface for each case can be shown using the plot of log[$Z^*(t)$] versus log(t) for each case. The interface shift, $Z^*(t)$, relative to the position of the interface at t=0 is calculated by using the definition of interface position; z^* is the position at ϕ_s=0.5 as in the Eq. (29). As anticipated, the movement of interface for G=2 is faster than the other. In the comparison of the interface movements for G=1 and G=2, the interface of G=2 moves farther from the initial front than that of G=1 for the same time step. Since the case of G=2 is the interdiffusion of a dissimilar polymer pair with more different monomeric friction coefficients between each component than those of the G=1 case, we can predict that a bigger discrepancy in physical property between each polymer, especially in the monomeric friction coefficient, means a faster interface movement, that is, a faster swelling. The time dependence of the interfacial width $W(t)$, is shown in Figure 9 with the plot of the log[$W(t)$] versus log(t) for each case. The interfacial width of G=2 from the initial sharp front increases by greater amount than that of G=1. In Figure 10, the plot of the log[$M(t)$] versus log(t) for each case is shown. For the time evolution of $M(t)$, the similar

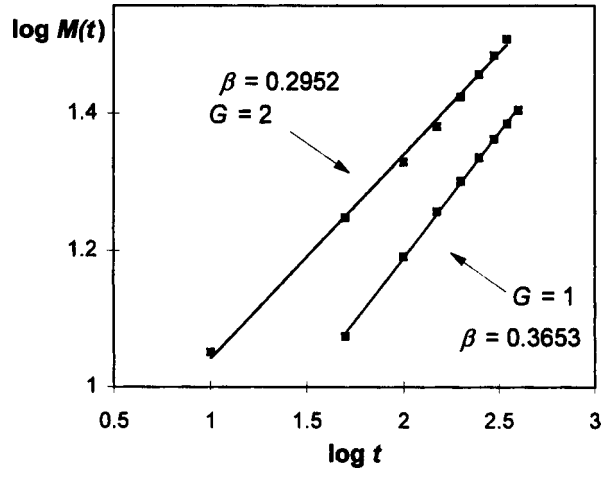

Figure 10. Comparison of the time dependence of the mass transport, $M(t)$ for G=2, R=1, N=3 with that for G=1, R=1, N=3 at consecutive times, plotted in the double-logarithmic form, that is, the plot of log[$M(t)$] versus log(t). The slope α is 0.2952, 0.3653 for G=2, G=1, respectively.

behavior can be found, that is, the mass transport $M(t)$ of G=2 increases faster than that of G=1.

Here, two interesting behaviors can be found. The first behavior of interest is that the magnitudes of the exponents α and β decrease as the G value increases. The values of α are 0.2638, 0.2404 and the values of β are 0.3653, 0.3133, for G=1, G=2, respectively. Comparing these results with the value of α and β for the similar polymer case of R=0 and G=0 (α=0.461 and β=0.4588), this tendency is clear. Even though the interfacial width $W(t)$ and the mass transport across the interface $M(t)$ are enlarged in proportion to the difference of physical properties between polymer components, the components are saturated quicker to a stable interface of finite width, that is to say, if the value of G becomes greater, then more non-Fickian characteristics can be

found. It is the suppressed diffusion due to the spinodal barrier, so diffusion is not free with the system in the two-phase region or more restriction for penetration. The second interest-holding result is the smaller value of α than 0.25, that is 0.2489, 0.2404, for G=1, G=2, respectively. From a simple dimensional analysis, one tends to conclude that the exponent α has to fall between 1/4 (the Cahn-Hilliard term dominant[30]) and 1/2 (the Fickian characteristic). But competition and balance between interfacial and thermodynamic forces may lead to a much smaller α than the "lower bound" 0.25. From Klein's data for interdiffusion between two partially miscible polymers (PS/d-PS), the exponent α is evaluated to be 0.21. And the studies of S. Q. Wang *et al.* represented the range of 0.10-0.23 for α when β falls in the range of 0.37-0.41.[31] Evidently, both experiment and theory allowed α to be smaller than 0.25, at least for the definition of interfacial width specified by Eq. (29). The fact that α is smaller than 0.25 means that the exponent α alone cannot well characterize the entire transport process even when the system is near the critical point for complete mixing. It at best depicts how sharply the composition field varies across the interface. This indicates that the "uphill" diffusion represented by the third term on the right hand side of Eq. (27) is well balanced by the Cahn-Hilliard interfacial effect described by the fourth term in Eq. (27). This explains why the exponent has become so small, even falling below 0.25.

Conclusion

We have studied the phenomena of interdiffusion at interfaces of dissimilar polymers from a theoretical viewpoint by deriving a dynamic model for collective interdiffusion and spinodal decomposition in polymeric materials. The model was applied to the polymer pairs with similar properties and to polymer pairs with very dissimilar physical properties to predict the concentration profile at the interfaces. Since the friction coefficients are highly composition dependent, the concentration profiles have different forms for the different values of G. In the case of dissimilar polymer pairs, the concentration profiles were asymmetric, with a substantial swelling of the slower-diffusing phase as a swelling front, and can be compared with symmetric cases. Using this model, the time dependent properties, $W(t)$, $M(t)$, and $Z^*(t)$ can be calculated. And the tendency of these properties for each G value is shown. Our predictions agree well with the available experimental data. Nevertheless, we point out that the time dependence of the interfacial width $W(t)$ alone is not sufficient to fully characterize the transport process. We predict in our calculation that $W(t)$ stop broadening after a sufficiently long time period and loses its function as a monitor of the interdiffusion process. Also, during a certain period when a power law such as $W(t)$ holds, it is found that α is actually smaller than 0.25, in agreement with some experimental data. The other quantities such as the mass transport $M(t)$ and the distance of interface $Z^*(t)$ replace the function of $W(t)$ to provide an illustration of interdiffusive transport.

It is necessary to improve our calculation for more reliable results. For example, we need the higher skills of numerical method to describe the interdiffusion phenomena for a long time stage.

Acknowledgment. The present studies were supported (in part) by the Basic Science Research Institute Program, Ministry of Education, 1996, Project No. BSRI-96-3414.

References

1. Kausch, H. H.; Tirrell, M. *Annu. Rev. Mater. Sci.* **1989**, *19*, 341.
2. Sauer, B. B.; Walsh, D. J. *Macromolecules* **1991**, *24*, 5948.
3. Brochard-Wyart, F.; de Gennes, P. G. *Makromol. Chem., Makromol. Symp.* **1990**, *40*, 167.
4. Brochard-Wyart, F. *Proc. Toyota Conf. Stud. Polym. Sci.* **1988**, *2*, 249.
5. Jabbari, E.; Peppas, N. A. *Macromolecules* **1993**, *21*, 1513.
6. Chaturvedi, U. K.; Steiner, U.; Zak, O.; Krausch, G.; Klein, *J. Phys. Rev. Lett.* **1989**, *63*, 616.
7. Steiner, U.; Kraush, G.; Schatz, G.; Klein, *J. Phys. Rev. Lett.* **1990**, *64*, 1119
8. de Gennes, P. G. *Scaling Concepts in Polymer Physics*; Cornell University Press: Ithaca, New York, 1979.
9. Tead, S. F.; Kramer, E. J. *Macromolecules* **1988**, *21*, 235.
10. Green, P. F.; Palmstrom, C. J.; Mayer, J. W.; Kramer, E. J. *Macromolecules* **1985**, *18*, 501.
11. Kramer, E. J.; Green, P. F.; Palmstrim, C. J. *Polymer* **1984**, *25*, 473.
12. Sillescu, H. *Makromol. Chem., Rapid Commun.* **1987**, *8*, 393.
13. Ascacu, A. Z.; Nagele, G.; Klein, R. *Macromolecules* **1990**, *24*, 4408.
14. Cussler, E. L. *Multicomponent Diffusion*; Elsevier: Amsterrdam, 1976; p 1.
15. Reiter, G.; Huttenbash, S.; Foster, M.; Stamm, M. *Macromolecules* **1991**, *24*, 1179.
16. Composto, R. J.; Kramer, E. J. *J. Mater. Sci.* **1992**, *26*, 2815.
17. Onasger, L. *Ann. NY Acad. Sci.* **1933**, *34*, 241.
18. Onasger, L. *Phys. Rev.* **1931**, *37*, 405.
19. Jabbari, E.; Peppas, N. A. *J. Mater. Sci.* **1994**, *29*, 3969.
20. Flory, P. J. *Principles of Polymer Chemistry*; Cornell University Press: Ithaca, NY, 1953; p 495.
21. Helfand, E.; Tagami, Y. *J. Chem. Phys.* **1971**, *56*, 3592. Hefand, E.; Sapse, A. M. *J. Chem. Phys.* **1975**, *62*, 1327.
22. Leibler, L. *Macromolecules* **1982**, *15*, 1238.
23. De Gennes, P. G. *J. Chem. Phys.* **1980**, *72*, 4756.
24. Binder, K. *J. Chem. Phys.* **1983**, *79*, 6837.
25. Jilge, W.; Carmesin, I.; Kremer, K.; Binder, K. *Macromolecules* **1990**, *23*, 5001.
26. Roland, C. M.; Ngai, K. L. *Macromolecules* **1992**, *25*, 363.
27. E. Jabbari, N. A. *Peppas, polymer* **1995**, *36*, 575.
28. Green, P. F.; Adolf, D. B.; Gilliom, L. R. *Macromolecules* **1991**, *24*, 3377.
29. Creton, C.; Kramer, E. J.; Hul, C. Y.; Brown, H. R. *Macromolecules* **1992**, *25*, 3705.
30. Cahn, J. W.; Hilliad, J. E. *J. Chem. Phys.* **1958**, *28*, 258. Cahn, J. W. *Acta Metall.* **1961**, *9*, 795.
31. Wang, S. Q.; Shi, Q. H. *Macromolecules* **1993**, *26*, 1091.